

Proceedings of the 12<sup>th</sup> International Conference on  
Computational Fluid Dynamics in the Oil & Gas,  
Metallurgical and Process Industries

# Progress in Applied CFD – CFD2017



SINTEF Proceedings

Editors:

Jan Erik Olsen and Stein Tore Johansen

## **Progress in Applied CFD – CFD2017**

Proceedings of the 12<sup>th</sup> International Conference on Computational Fluid Dynamics  
in the Oil & Gas, Metallurgical and Process Industries

SINTEF Academic Press

SINTEF Proceedings no 2

Editors: Jan Erik Olsen and Stein Tore Johansen

**Progress in Applied CFD – CFD2017**

Selected papers from 10<sup>th</sup> International Conference on Computational Fluid Dynamics in the Oil & Gas, Metallurgical and Process Industries

Key words:

CFD, Flow, Modelling

Cover, illustration: Arun Kamath

ISSN 2387-4295 (online)

ISBN 978-82-536-1544-8 (pdf)

© Copyright SINTEF Academic Press 2017

The material in this publication is covered by the provisions of the Norwegian Copyright Act. Without any special agreement with SINTEF Academic Press, any copying and making available of the material is only allowed to the extent that this is permitted by law or allowed through an agreement with Kopinor, the Reproduction Rights Organisation for Norway. Any use contrary to legislation or an agreement may lead to a liability for damages and confiscation, and may be punished by fines or imprisonment

SINTEF Academic Press

Address:       Forskningsveien 3 B  
                  PO Box 124 Blindern  
                  N-0314 OSLO

Tel:             +47 73 59 30 00

Fax:             +47 22 96 55 08

[www.sintef.no/byggforsk](http://www.sintef.no/byggforsk)

[www.sintefbok.no](http://www.sintefbok.no)

**SINTEF Proceedings**

SINTEF Proceedings is a serial publication for peer-reviewed conference proceedings on a variety of scientific topics.

The processes of peer-reviewing of papers published in SINTEF Proceedings are administered by the conference organizers and proceedings editors. Detailed procedures will vary according to custom and practice in each scientific community.

## PREFACE

This book contains all manuscripts approved by the reviewers and the organizing committee of the 12th International Conference on Computational Fluid Dynamics in the Oil & Gas, Metallurgical and Process Industries. The conference was hosted by SINTEF in Trondheim in May/June 2017 and is also known as CFD2017 for short. The conference series was initiated by CSIRO and Phil Schwarz in 1997. So far the conference has been alternating between CSIRO in Melbourne and SINTEF in Trondheim. The conferences focuses on the application of CFD in the oil and gas industries, metal production, mineral processing, power generation, chemicals and other process industries. In addition pragmatic modelling concepts and bio-mechanical applications have become an important part of the conference. The papers in this book demonstrate the current progress in applied CFD.

The conference papers undergo a review process involving two experts. Only papers accepted by the reviewers are included in the proceedings. 108 contributions were presented at the conference together with six keynote presentations. A majority of these contributions are presented by their manuscript in this collection (a few were granted to present without an accompanying manuscript).

The organizing committee would like to thank everyone who has helped with review of manuscripts, all those who helped to promote the conference and all authors who have submitted scientific contributions. We are also grateful for the support from the conference sponsors: ANSYS, SFI Metal Production and NanoSim.

Stein Tore Johansen & Jan Erik Olsen



Organizing committee:

Conference chairman: Prof. Stein Tore Johansen

Conference coordinator: Dr. Jan Erik Olsen

Dr. Bernhard Müller

Dr. Sigrid Karstad Dahl

Dr. Shahriar Amini

Dr. Ernst Meese

Dr. Josip Zoric

Dr. Jannike Solsvik

Dr. Peter Witt

Scientific committee:

Stein Tore Johansen, SINTEF/NTNU

Bernhard Müller, NTNU

Phil Schwarz, CSIRO

Akio Tomiyama, Kobe University

Hans Kuipers, Eindhoven University of Technology

Jinghai Li, Chinese Academy of Science

Markus Braun, Ansys

Simon Lo, CD-adapco

Patrick Segers, Universiteit Gent

Jiyuan Tu, RMIT

Jos Derksen, University of Aberdeen

Dmitry Eskin, Schlumberger-Doll Research

Pär Jönsson, KTH

Stefan Pirker, Johannes Kepler University

Josip Zoric, SINTEF

## CONTENTS

<b>PRAGMATIC MODELLING .....</b>	<b>9</b>
On pragmatism in industrial modeling. Part III: Application to operational drilling .....	11
CFD modeling of dynamic emulsion stability .....	23
Modelling of interaction between turbines and terrain wakes using pragmatic approach .....	29
<b>FLUIDIZED BED .....</b>	<b>37</b>
Simulation of chemical looping combustion process in a double looping fluidized bed reactor with cu-based oxygen carriers.....	39
Extremely fast simulations of heat transfer in fluidized beds.....	47
Mass transfer phenomena in fluidized beds with horizontally immersed membranes .....	53
A Two-Fluid model study of hydrogen production via water gas shift in fluidized bed membrane reactors .....	63
Effect of lift force on dense gas-fluidized beds of non-spherical particles .....	71
Experimental and numerical investigation of a bubbling dense gas-solid fluidized bed .....	81
Direct numerical simulation of the effective drag in gas-liquid-solid systems .....	89
A Lagrangian-Eulerian hybrid model for the simulation of direct reduction of iron ore in fluidized beds.....	97
High temperature fluidization - influence of inter-particle forces on fluidization behavior .....	107
Verification of filtered two fluid models for reactive gas-solid flows .....	115
<b>BIOMECHANICS.....</b>	<b>123</b>
A computational framework involving CFD and data mining tools for analyzing disease in carotid artery .....	125
Investigating the numerical parameter space for a stenosed patient-specific internal carotid artery model.....	133
Velocity profiles in a 2D model of the left ventricular outflow tract, pathological case study using PIV and CFD modeling.....	139
Oscillatory flow and mass transport in a coronary artery.....	147
Patient specific numerical simulation of flow in the human upper airways for assessing the effect of nasal surgery.....	153
CFD simulations of turbulent flow in the human upper airways .....	163
<b>OIL &amp; GAS APPLICATIONS .....</b>	<b>169</b>
Estimation of flow rates and parameters in two-phase stratified and slug flow by an ensemble Kalman filter .....	171
Direct numerical simulation of proppant transport in a narrow channel for hydraulic fracturing application .....	179
Multiphase direct numerical simulations (DNS) of oil-water flows through homogeneous porous rocks .....	185
CFD erosion modelling of blind tees .....	191
Shape factors inclusion in a one-dimensional, transient two-fluid model for stratified and slug flow simulations in pipes .....	201
Gas-liquid two-phase flow behavior in terrain-inclined pipelines for wet natural gas transportation .....	207

<b>NUMERICS, METHODS &amp; CODE DEVELOPMENT .....</b>	<b>213</b>
Innovative computing for industrially-relevant multiphase flows .....	215
Development of GPU parallel multiphase flow solver for turbulent slurry flows in cyclone.....	223
Immersed boundary method for the compressible Navier–Stokes equations using high order summation-by-parts difference operators .....	233
Direct numerical simulation of coupled heat and mass transfer in fluid-solid systems .....	243
A simulation concept for generic simulation of multi-material flow, using staggered Cartesian grids.....	253
A cartesian cut-cell method, based on formal volume averaging of mass, momentum equations.....	265
SOFT: a framework for semantic interoperability of scientific software .....	273
<b>POPULATION BALANCE .....</b>	<b>279</b>
Combined multifluid-population balance method for polydisperse multiphase flows .....	281
A multifluid-PBE model for a slurry bubble column with bubble size dependent velocity, weight fractions and temperature.....	285
CFD simulation of the droplet size distribution of liquid-liquid emulsions in stirred tank reactors .....	295
Towards a CFD model for boiling flows: validation of QMOM predictions with TOPFLOW experiments .....	301
Numerical simulations of turbulent liquid-liquid dispersions with quadrature-based moment methods.....	309
Simulation of dispersion of immiscible fluids in a turbulent couette flow .....	317
Simulation of gas-liquid flows in separators - a Lagrangian approach.....	325
CFD modelling to predict mass transfer in pulsed sieve plate extraction columns .....	335
<b>BREAKUP &amp; COALESCENCE .....</b>	<b>343</b>
Experimental and numerical study on single droplet breakage in turbulent flow .....	345
Improved collision modelling for liquid metal droplets in a copper slag cleaning process .....	355
Modelling of bubble dynamics in slag during its hot stage engineering.....	365
Controlled coalescence with local front reconstruction method .....	373
<b>BUBBLY FLOWS .....</b>	<b>381</b>
Modelling of fluid dynamics, mass transfer and chemical reaction in bubbly flows .....	383
Stochastic DSMC model for large scale dense bubbly flows.....	391
On the surfacing mechanism of bubble plumes from subsea gas release.....	399
Bubble generated turbulence in two fluid simulation of bubbly flow .....	405
<b>HEAT TRANSFER .....</b>	<b>413</b>
CFD-simulation of boiling in a heated pipe including flow pattern transitions using a multi-field concept .....	415
The pear-shaped fate of an ice melting front .....	423
Flow dynamics studies for flexible operation of continuous casters (flow flex cc).....	431
An Euler-Euler model for gas-liquid flows in a coil wound heat exchanger.....	441
<b>NON-NEWTONIAN FLOWS.....</b>	<b>449</b>
Viscoelastic flow simulations in disordered porous media .....	451
Tire rubber extrudate swell simulation and verification with experiments .....	459
Front-tracking simulations of bubbles rising in non-Newtonian fluids.....	469
A 2D sediment bed morphodynamics model for turbulent, non-Newtonian, particle-loaded flows.....	479

<b>METALLURGICAL APPLICATIONS.....</b>	<b>491</b>
Experimental modelling of metallurgical processes .....	493
State of the art: macroscopic modelling approaches for the description of multiphysics phenomena within the electroslag remelting process .....	499
LES-VOF simulation of turbulent interfacial flow in the continuous casting mold .....	507
CFD-DEM modelling of blast furnace tapping .....	515
Multiphase flow modelling of furnace tapholes .....	521
Numerical predictions of the shape and size of the raceway zone in a blast furnace.....	531
Modelling and measurements in the aluminium industry - Where are the obstacles? .....	541
Modelling of chemical reactions in metallurgical processes.....	549
Using CFD analysis to optimise top submerged lance furnace geometries .....	555
Numerical analysis of the temperature distribution in a martensic stainless steel strip during hardening.....	565
Validation of a rapid slag viscosity measurement by CFD.....	575
Solidification modeling with user defined function in ANSYS Fluent.....	583
Cleaning of polycyclic aromatic hydrocarbons (PAH) obtained from ferroalloys plant.....	587
Granular flow described by fictitious fluids: a suitable methodology for process simulations .....	593
A multiscale numerical approach of the dripping slag in the coke bed zone of a pilot scale Si-Mn furnace.....	599
 <b>INDUSTRIAL APPLICATIONS .....</b>	 <b>605</b>
Use of CFD as a design tool for a phosphoric acid plant cooling pond .....	607
Numerical evaluation of co-firing solid recovered fuel with petroleum coke in a cement rotary kiln: Influence of fuel moisture .....	613
Experimental and CFD investigation of fractal distributor on a novel plate and frame ion-exchanger .....	621
 <b>COMBUSTION .....</b>	 <b>631</b>
CFD modeling of a commercial-size circle-draft biomass gasifier.....	633
Numerical study of coal particle gasification up to Reynolds numbers of 1000.....	641
Modelling combustion of pulverized coal and alternative carbon materials in the blast furnace raceway .....	647
Combustion chamber scaling for energy recovery from furnace process gas: waste to value .....	657
 <b>PACKED BED.....</b>	 <b>665</b>
Comparison of particle-resolved direct numerical simulation and 1D modelling of catalytic reactions in a packed bed .....	667
Numerical investigation of particle types influence on packed bed adsorber behaviour .....	675
CFD based study of dense medium drum separation processes .....	683
A multi-domain 1D particle-reactor model for packed bed reactor applications.....	689
 <b>SPECIES TRANSPORT &amp; INTERFACES .....</b>	 <b>699</b>
Modelling and numerical simulation of surface active species transport - reaction in welding processes .....	701
Multiscale approach to fully resolved boundary layers using adaptive grids.....	709
Implementation, demonstration and validation of a user-defined wall function for direct precipitation fouling in Ansys Fluent.....	717



<b>FREE SURFACE FLOW &amp; WAVES .....</b>	<b>727</b>
Unresolved CFD-DEM in environmental engineering: submarine slope stability and other applications.....	729
Influence of the upstream cylinder and wave breaking point on the breaking wave forces on the downstream cylinder .....	735
Recent developments for the computation of the necessary submergence of pump intakes with free surfaces .....	743
Parallel multiphase flow software for solving the Navier-Stokes equations .....	752
 <b>PARTICLE METHODS .....</b>	 <b>759</b>
A numerical approach to model aggregate restructuring in shear flow using DEM in Lattice-Boltzmann simulations .....	761
Adaptive coarse-graining for large-scale DEM simulations.....	773
Novel efficient hybrid-DEM collision integration scheme.....	779
Implementing the kinetic theory of granular flows into the Lagrangian dense discrete phase model.....	785
Importance of the different fluid forces on particle dispersion in fluid phase resonance mixers .....	791
Large scale modelling of bubble formation and growth in a supersaturated liquid.....	798
 <b>FUNDAMENTAL FLUID DYNAMICS .....</b>	 <b>807</b>
Flow past a yawed cylinder of finite length using a fictitious domain method .....	809
A numerical evaluation of the effect of the electro-magnetic force on bubble flow in aluminium smelting process.....	819
A DNS study of droplet spreading and penetration on a porous medium.....	825
From linear to nonlinear: Transient growth in confined magnetohydrodynamic flows.....	831

## STOCHASTIC DSMC MODEL FOR LARGE SCALE DENSE BUBBLY FLOWS

Satish KAMATH<sup>1\*</sup>, Johan T. PADDING<sup>2</sup>, Kay A. BUIST<sup>1</sup>, J. A. M. KUIPERS<sup>1</sup>

<sup>1</sup>Multiphase Reactors Group, Department of Chemical Engineering & Chemistry, Eindhoven University of Technology, P.O. Box 513, 5600 MB Eindhoven, The Netherlands

<sup>2</sup>Process and Energy Department, Delft University of Technology, Building 34K Leeghwaterstraat 39  
2628 CB Delft, The Netherlands

\* E-mail: s.s.kamath@tue.nl

### ABSTRACT

Bubble columns are widely used in the chemical industry because of their simple design and high efficiency. The scale-up of these kinds of columns is challenging and time-consuming. Since high throughput is targeted, they are operated in the heterogeneous bubbling regime where the flow is complex and turbulent. Large-scale bubble columns can in principle be simulated using continuum models (TFM/MFM) with closures from more detailed models such as Front Tracking (FT) or Volume of Fluid (VOF). Multi-fluid models are capable of predicting the flow field, but to accurately describe mass transfer rates, an accurate interfacial area of the bubbles is required as well as mass transfer coefficients for dense bubble swarms. This requires the MFM to be coupled with models that can predict bubble size distributions. The Discrete Bubble Model (DBM) can be scaled up but the bubble-bubble interactions make it computationally very intensive.

Stochastic Direct Simulation Monte Carlo (DSMC) methods treat the bubbles in a discrete manner while more efficiently handling the collisions compared to the DBM. The DSMC model has earlier been used for very small particles in the size range of Angstroms to microns where the particles are purely inertial at high Stokes numbers. In the work of Pawar *et al.* (2014) this was used for micrometer sized particles/droplets where this method proved to be 60 to 70 times faster than more classical methods like the Discrete Particle Model (DPM).

In this work the DSMC method has been extended to finite sized bubbles/particles in the order of millimeters. A 4-way coupling (liquid-bubble-bubble) is achieved using the volume-averaged Navier Stokes equations. The model is verified first for mono-disperse impinging particle streams without gas. Then the model is verified with the DBM of a 3D periodic bubble driven system. The collision frequencies are all within 10 percent accuracy and the speed up achieved per DEM time step is nearly 10 times compared to the DBM, which facilitates simulation of large systems.

**Keywords:** Euler-Lagrange methods, bubble dynamics, optimization, stochastic methods, DSMC.

### NOMENCLATURE

#### Greek Symbols

$\rho$	Mass density, $[kg/m^3]$
$\mu$	Dynamic viscosity, $[kg/ms]$
$\varepsilon$	Porosity, $[-]$
$\tau$	Shear stress, $[N/m^2]$
$\phi$	Volumetric momentum source term, $[N/m^3]$

#### Latin Symbols

$\mathbf{F}$	Force (vector), $[N]$
$P$	Pressure, $[Pa]$
$\mathbf{u}$	Continuous phase velocity vector, $[m/s]$
$\mathbf{v}$	Discrete phase velocity vector, $[m/s]$
$\mathbf{g}$	Gravitational acceleration vector, $[m/s^2]$
$V$	Discrete phase volume, $[m^3]$
$R$	Bubble radius, $[m]$

#### Sub/superscripts

$b$	discrete phase
$l$	continuous phase
$L$	Laminar
$T$	Turbulent
$bub$	bubble
$flow$	flow

### INTRODUCTION

#### Bubble columns

Bubble column reactors are widely used as gas-liquid contactors in the chemical and energy industries. A wide variety of processes like absorption, fermentation, Fischer-Tropsch synthesis, waste water treatment, bio-reactors etc. are operated in bubble columns. The design of such columns is based on parameters such as throughput, conversion, type of reactions etc. The industrial grade columns with large throughputs have volumes in the range of 100-300  $m^3$ . Larger columns are also employed for bio-processes like fermentation (3000  $m^3$ ) and waste water treatment (20000  $m^3$ ) (Deen *et al.*, 2012).

Figure 1 shows a schematic representation of a bubble column. Often, bubble columns are equipped with internal parts, depending on the application. If the reaction is highly exothermic, cooling tubes will be present inside the column. Catalyst particles may also be suspended in the liquid phase to facilitate faster conversion of the reactants.

The bubble dynamics and bubble size distribution inside the column dictate the liquid phase flow. This in turn controls the rate of mass transfer from the bubble to the liquid phase and also the heat transfer with submerged heat exchange tubes. Modeling of such bubble columns is very challenging and typically empirical correlations (Chaudhari and Ramachandran, 1980) are used even today. Recent advances in computational power and techniques have made

it possible to simulate the flow structures in such columns which occur at multiple time and length scales.

### Multi-scale approach

A multi-scale approach can be employed to simulate the complex fluid flow in a bubble column (see figure 2). At the lowest level methods such as Front-Tracking (Unverdi and Tryggvason, 1992) and Volume of Fluid (van Sint Annaland *et al.*, 2005) methods are used to simulate the behaviour of a single bubble or a group of interacting bubbles rising through the liquid phase. An Euler-Lagrange approach, such as the Discrete Bubble Model (DBM), is used to simulate larger length and time scales. This method uses closures from the above methods because the flow field around a bubble is not completely resolved. The DBM is a suitable method to understand the influence of bubble-bubble interactions and bubble wall encounters on large scale flow structures. The method becomes computationally expensive when simulating dense bubbly flows because every bubble is tracked explicitly and the bubble-bubble encounters have to be resolved in time. Therefore, at the industrial scale, Euler-Euler approaches are used with closures from the intermediate scale (Deen *et al.*, 2004a).

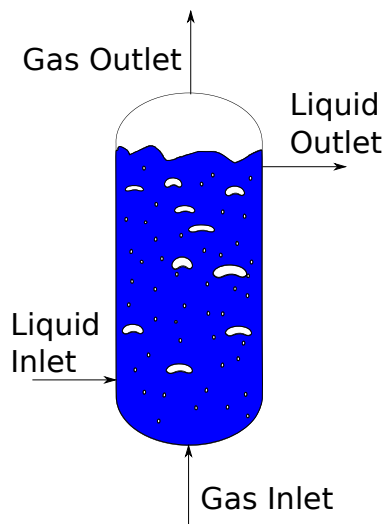


Figure 1: Schematic diagram of a bubble column.

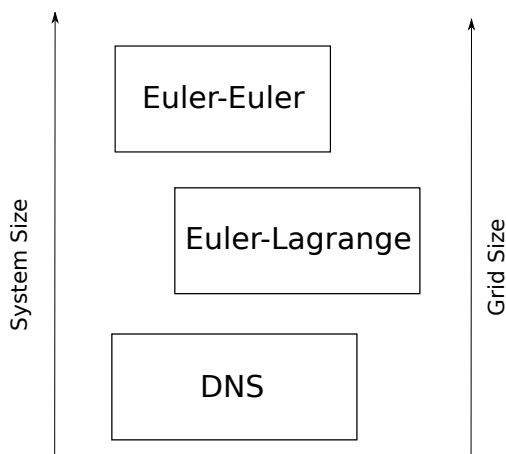


Figure 2: Multiscale approaches at different time and length scales.

### Problems with Euler-Euler approach

Euler-Euler approaches such as the Multi Fluid Model represent the bubble phase with different size classes. Coupled conservation equations are solved for each size class with suitable closures. The interactions among the different considered phases need to be explicitly defined. Bubble-bubble interactions are not accounted for nor the naturally occurring phenomena of coalescence and break-up. Dedicated external models, such as the population balance models, have to be integrated with the Multi-Fluid Model to account for coalescence and break-up (Zhang, 2007). In the work of (Zhang, 2007) the range of bubble sizes is assumed to be 2-4 mm while the other parameters such as drag, lift etc. are assumed to not vary much. Therefore a two-fluid approach is employed. This limits the range of bubble size, which influences the dynamics of the column.

### Objective

The main objective of this work is to develop an Euler-Lagrange model that can be used for large scale simulation of bubble columns (10-100  $m^3$ ). Bubble-bubble and bubble-wall interactions are one of the bottlenecks in the computational speed of the simulation. Therefore to resolve this issue, a stochastic Direct Simulation Monte-Carlo (DSMC) approach is used to execute the collisions. Pawar *et al.* (2014) and Du *et al.* (2011) have shown that the method is nearly two orders of magnitude faster than the DBM, but there are limitations to the approach with respect to the length scale of the simulation and the volume fraction of the discrete phase (Pawar *et al.*, 2014). This work aims to extend the DSMC approach to larger object sizes (in the order of millimeters) and to resolve the volume fraction limitation. Furthermore, this work aims to extend the method so that it can handle bubble-bubble collisions efficiently. Addition of a fluid phase where the fluid phase forces also contribute considerably to the bubble dynamics, adds an extra level of complexity because these have to be considered in the calculation of the collision frequency.

In the next sections, the method is briefly described and the model verification results are presented.

### MODEL DESCRIPTION

#### Discrete phase

DSMC methods are normally associated with a parcel approach where a group of discrete objects are represented by one simulated object. The systems for which this method was developed are molecular systems that have finite/large Knudsen number (Bird, 1994). In this work the DSMC method has been extended to larger discrete phase sizes (in the order of millimeters) with low Knudsen number. For simplicity a parcel size 1 is chosen, but in future work we will also explore larger parcel sizes. The bubbles are tracked individually where the momentum equations (see equations 1 and 2) need to be solved to obtain new velocities of the particles. Pawar *et al.* (2014) have reported a major speed boost with the DSMC model compared to the discrete particle approach with the same parcel size.

The bubble is assumed to be incompressible and the density of the bubble is also assumed to be constant. Forces considered here are gravitational ( $F_G$ ), pressure ( $F_P$ ), drag ( $F_D$ ),

lift ( $\mathbf{F}_L$ ), virtual mass ( $\mathbf{F}_{VM}$ ) and wall lubrication ( $\mathbf{F}_W$ ) (see equation 2).

$$\rho_b V_b \frac{d(\mathbf{v})}{dt} = \Sigma \mathbf{F} - (\rho_b \frac{d(V_b)}{dt}) \mathbf{v} \quad (1)$$

$$\Sigma \mathbf{F} = \mathbf{F}_G + \mathbf{F}_p + \mathbf{F}_D + \mathbf{F}_L + \mathbf{F}_{VM} + \mathbf{F}_W \quad (2)$$

The drag, lift and wall forces used here are from Tomiyama *et al.* (1995, 2002). The drag correction for bubble swarms is included from Roghair *et al.* (2011). A more detailed explanation about the forces and closures used can be found in works of Darmana *et al.* (2006); Jain *et al.* (2014).

### Liquid phase hydrodynamics

The liquid phase dynamics are described by the volume averaged Navier-Stokes equations coupled with the continuity equation (see equations 3 and 4).

$$\frac{\partial(\varepsilon_l \rho_l)}{\partial t} + \nabla \cdot \varepsilon_l \rho_l \mathbf{u} = 0 \quad (3)$$

$$\frac{\partial(\varepsilon_l \rho_l \mathbf{u})}{\partial t} + \nabla \cdot \varepsilon_l \rho_l \mathbf{u} \mathbf{u} = -\varepsilon_l \nabla P - \nabla \cdot \varepsilon_l \boldsymbol{\tau}_l + \varepsilon_l \rho_l \mathbf{g} + \phi \quad (4)$$

$\varepsilon_l$  represents the local liquid fraction and  $\phi$  represents the local momentum source term for the force exerted by the bubbles on the liquid. The shear stress term  $\boldsymbol{\tau}_l$  is given by:

$$\boldsymbol{\tau}_l = -\mu_{eff,l}((\nabla \mathbf{u}) + (\nabla \mathbf{u})^T - \frac{2}{3} \mathbf{I}(\nabla \cdot \mathbf{u})) \quad (5)$$

where

$$\mu_{eff,l} = \mu_{L,l} + \mu_{T,l} \quad (6)$$

$\mu_{T,l}$  arises from the convection term when the Navier-Stokes equations are volume averaged and the Boussinesq eddy viscosity assumption. Deen *et al.* (2001) have compared different turbulence models with experimental data in the Euler-Euler framework for a square bubble column. They concluded that the large eddy simulation outperforms the  $k-\varepsilon$  model. Therefore, the same framework as Deen *et al.* (2001) was chosen for the liquid phase.  $\mu_{T,l}$  is closed with the sub-grid scale eddy viscosity expression given by Vreman (2004):

$$\mu_{T,l} = \rho_l c \sqrt{\frac{\beta_b}{\alpha_{ij} \alpha_{ij}}} \quad (7)$$

**Table 1:** Terms in the Vreman SGS model. Vreman (2004)

Term	Definition
$c$	$2.5 C_s^2$
$\alpha_{ij}$	$\frac{\partial \bar{u}_j}{\partial x_i}$
$\beta_{ij}$	$\Delta_m^2 \alpha_{mi} \alpha_{mj}$
$\beta_b$	$\beta_{11} \beta_{22} - \beta_{12}^2 + \beta_{11} \beta_{33} - \beta_{13}^2 + \beta_{22} \beta_{33} - \beta_{23}^2$

where  $C_s$  is the Smagorinsky constant, the rest of the parameters are given by table 1. A similar approach has been used by Darmana *et al.* (2006) and also by Jain *et al.* (2014).

## NUMERICAL SOLUTION METHOD

### Time marching

In most of the Euler-Lagrangian frameworks the discrete and the continuous phases are time-marched in an alternate fashion with intermediate coupling. Therefore there is a flow time-step  $\delta t_{flow}$  and a bubble time-step  $\delta t_{bub}$ .  $\delta t_{flow}$  is divided into a fixed number of sub-steps of duration  $\delta t_{bub}$ . During  $\delta t_{bub}$ , the forces acting on each bubble are recalculated based on the local Eulerian flow-field. The bubble time-step  $\delta t_{bub}$  can be divided into several more time steps based on the collision frequency calculated for every bubble. More details about this are given in the section "Discrete phase dynamics".

The major difference in time marching between the deterministic approach employed by Darmana *et al.* (2006) and the stochastic approach used in this work is the resolution of the lowest time scale. In the deterministic approach, the collision times are explicitly calculated and a list is maintained to sequentially perform the collisions in the ascending order of their collision times. In the stochastic approach, the collision times are not determined, but rather collisions take place based on a probabilistic approach. This is described with more details in section "Discrete phase dynamics".

### Coupling

The coupling between the phases dictates the flow field in the column. Therefore the mapping procedure between the grid cells has to be considered carefully. Kitagawa *et al.* (2001) have proposed to use a Lagrangian template function for the volume fraction of the dispersed phase. Similarly Deen *et al.* (2004b) proposed a fourth order polynomial function for mapping the forces and volume fraction. The width of the distribution is set based on the bubble size. This makes the mapping independent of the size of the Eulerian grid. Darmana *et al.* (2006) have also used it for their Discrete Bubble Model. This mapping is implemented in this work and is also suitable for comparison with the Discrete Bubble Model.

Lau *et al.* (2011) have performed an extensive parametric study for different mapping window sizes for the polynomial function in a bubble column. They found that the size of the mapping window does not have an effect on the predicted mean and fluctuating velocities when a drag correction is used that uses local gas fraction. Therefore a mapping window of  $2R_{bub}$  is used.

### Discrete phase dynamics

The discrete phase equations are solved using a first order explicit scheme for equation 1:

$$\mathbf{v}^{n+1} = \frac{\Sigma \mathbf{F}^n}{m_b} \delta t_{bub} + \mathbf{v}^n \quad (8)$$

The forces are mapped from the Eulerian grid cells based on the polynomial function method described in the previous section. Then the bubble dynamics is treated adapting the algorithm shown in Pawar *et al.* (2014) with a few important modifications described later in this section. Once the bubble marching along with the collisions are treated, the Lagrangian forces are collected in the volumetric momentum source term  $\phi$ . This is repeated until the discrete phase has moved for a full  $\delta t_{flow}$ . From the new bubble positions, the bubble volume fractions are computed and subsequently

mapped back to the Eulerian domain to determine  $\epsilon_l$ .

During every bubble time step, the bubbles are marched forward in time by  $\delta t_{bub}$ . The collisions that occur during this time interval can introduce a big computational overhead for a large scale system with bubbles/particles in the order of millions. The algorithm of a deterministic model like the Discrete Bubble Model (Darmana *et al.*, 2006) is inherently serial as the collisions need to occur in the order of their collision times. These collision-times are maintained in an encounter list and the minimum time needs to be searched every time a collision occurs due to changes in bubble positions and velocities. This implies a large overhead for dense systems, even with the implementation of efficient neighbour list concepts.

The speed-up in the DSMC algorithm is mainly due to choosing a collision partner using probabilistic rules. There are several methods used for choosing the right collision pairs in DSMC such as the time counter method, Nanbu method, modified Nanbu method (Lutišan, 1995). Pawar *et al.* (2014) and Du *et al.* (2011) have used the modified Nanbu method with their own modifications for the searching scope and collision conditions.

As the flow becomes more dense, the Knudsen number becomes smaller. In such situations the local relative velocities between bubbles are also comparatively small. Therefore they tend to continuously collide due to less availability of interstitial space, therefore a structural factor must be included in the algorithm. This factor is the radial distribution function at contact ( $g(r)_{contact}$ ).

The DSMC algorithm performs collisions in a stochastic manner with neighbouring particles located within a defined searching scope. The expression for the probability ( $P_{ij}$ ) that a particle  $i$  collides with another particle  $j$  defined within its searching scope is given by:

$$P_{ij} = \frac{|\mathbf{v}|_{ij} \sigma \Delta t_p}{V_{s,i}} g(r)_{contact} \quad (9)$$

where  $|\mathbf{v}|_{ij}$  is the relative velocity magnitude between the two particles,  $\sigma$  is the cross-sectional areas of the collision cylinder which is computed from the sum of the projected cross sectional area of the two particles,  $\Delta t_p$  is the time step and  $V_{s,i}$  is the volume of the searching scope of the particle with index  $i$ . It can be shown that for a given particle size, a minimum relative velocity is needed for the probability to be valid based on the Nanbu method. To account for relative velocities much lower than the limit, a nearest neighbour collision algorithm is included. The nearest neighbour is the most likely collision partner for an entity in a dynamic system (Bird, 2007). This was implemented without hampering the speed of the already existing algorithm.

The collisions are executed using the hard sphere model (Hoomans *et al.*, 1996) once the collision pairs are chosen. The normal component of the momentum is simply exchanged between the two bubbles/particles and the tangential component is retained.

### Liquid phase numerical scheme

The continuity equation and the momentum equations are solved in a coupled manner using SIMPLE (Patankar, 1980).

The unsteady part is discretized using the first order Euler scheme. The convective fluxes in the continuity equation are treated implicitly. The convective, diffusive and the source terms are treated explicitly in the momentum equations.

## VERIFICATION AND RESULTS

The Discrete Bubble Model from Darmana *et al.* (Darmana *et al.*, 2006) is taken as the verification model. The model is verified through two problems:

1. Impinging particle streams (P1)
2. 3D - periodic bubble rise from rest (P2)

System P1 consists of two nozzles facing each other at an angle (see figure 3). The solid particles flow through these nozzles, collide and spread across the domain based on the outcome of the collisions. There is no interstitial fluid phase for this test case, therefore the velocity field of the particles is purely set by the collisions. The mass flow-rate is set for each nozzle (see table 2). The parameters are the mean particle velocities and the standard deviation of the velocities. A Gaussian distribution is used to generate velocities in x and z direction with given mean velocity and standard deviation. The mean of the velocity in the y direction is 0.

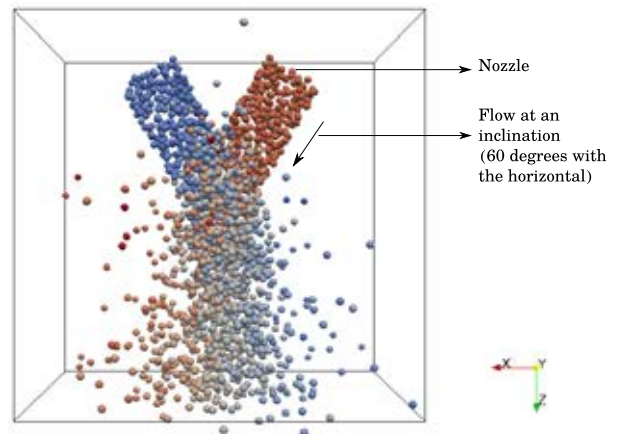


Figure 3: Schematic of the system for P1.

The 3D periodic system in P2 consists of an array of regularly spaced bubbles (see figure 4). The spacing between the bubbles is a little larger near the periodic planes than in the bulk of the domain. Therefore, there is a bias in bubble concentration towards the center. The bubbles start from rest and are coupled with an interstitial Newtonian liquid. Properties of air are used for the gas phase and water for the liquid phase.

### Impinging particle streams (P1)

The parameter space is defined in table 2. The DSMC collisions are velocity dependent. Therefore it is necessary to test the model at different velocity regimes. By changing the standard deviation of velocities we change the solid fraction at the impact region. Therefore two values for velocity standard deviations are chosen: one with the same order of magnitude as that of the mean velocity and one which is several orders of magnitude lower than the mean velocity. In

**Table 2:** Parameter space for particle size 2 mm.

Case	Mean velocity [m/s]	Std. deviation [m/s]	Mass flow rate [kg/s]
1	0.2	0.001	0.01
2	0.2	0.15	0.01
3	2.5	0.001	0.1
4	2.5	1.0	0.1

all cases, the total collisions and the collision frequency is measured for the entire domain.

The results are compared with the results obtained from the equivalent deterministic model. These are presented in figures 5 and 6. The initial condition is such that there are no particles in the domain. At  $t = 0$  the particles start flowing through the nozzles. They collide at the impact region and disperse, quickly achieving steady state.

The collision frequency increases exponentially initially and then reaches a steady state. The impact times of both streams match perfectly with the deterministic approach. The collision frequency in case 3 is over-predicted by about 5% compared to the equivalent DPM simulation. Since the DSMC smears out the collision window within its searching scope the size of the stochastic impact region in dense cases is slightly bigger than it actually is. Therefore, it takes into account some extra collisions.

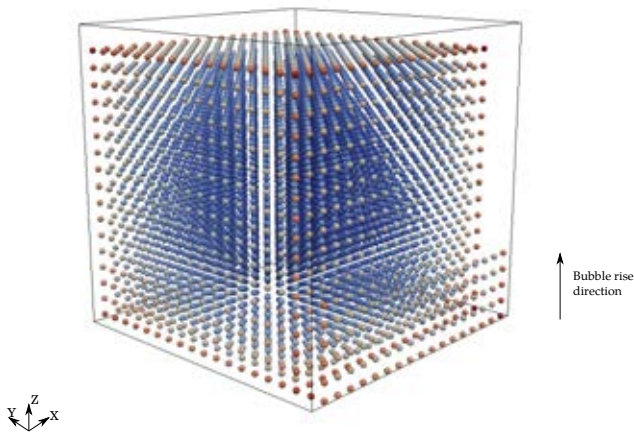


**Figure 4:** Schematic of the system for P2.

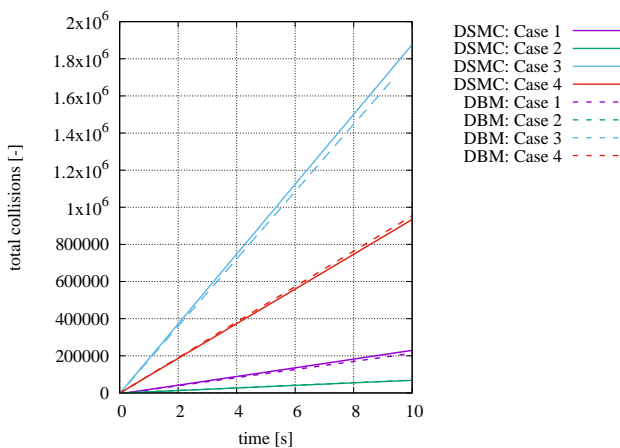


**Figure 5:** Total number of collisions occurring in the domain vs time for different cases, DBM vs DSMC.

### 3D-periodic bubble rise (P2)

The bubble rise starts from rest, with the initial condition as in figure 4. The bubbles rising in the wake of other bubbles experience less drag and tend to collide with the bubbles above them, pushing them forward. The bubbles act as small momentum sources at different locations in the domain and since the source terms are small the system needs some time before it reaches high velocities. This allows us to ob-

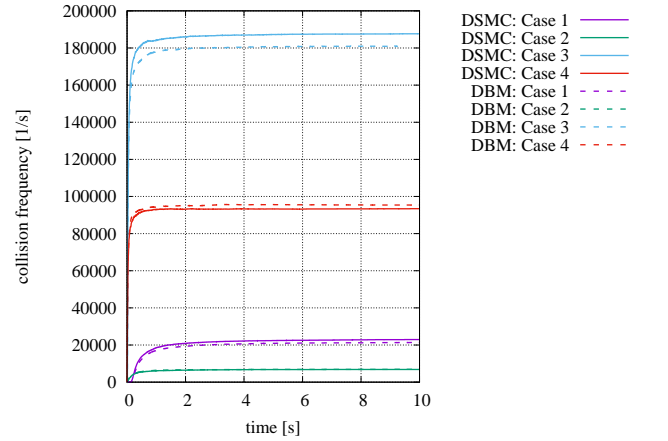


**Figure 6:** Collision frequency vs time for different cases, DBM vs DSMC.

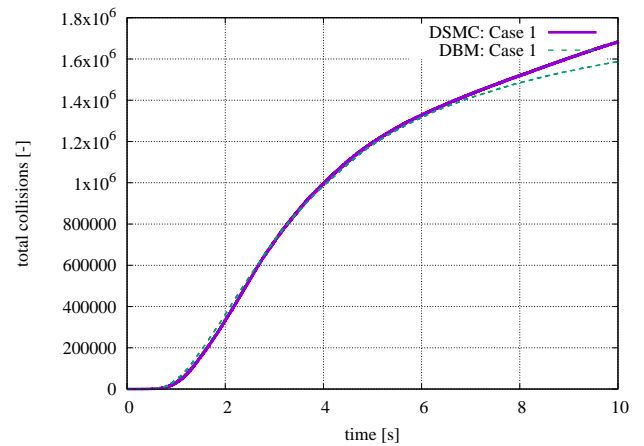


**Figure 7:** Total collisions occurring in domain vs time for different cases, DBM vs DSMC.

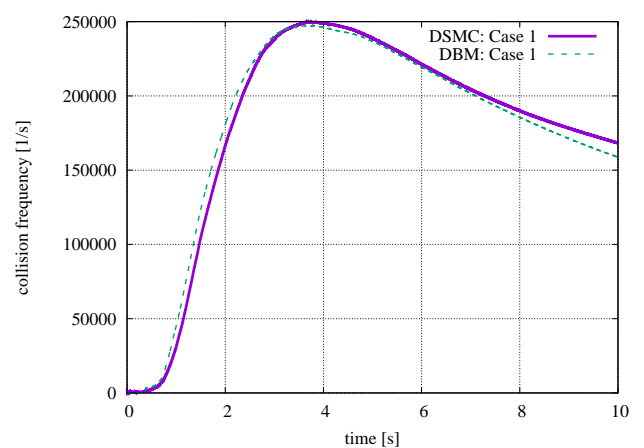


**Figure 8:** Collision frequency vs time for different cases, DBM vs DSMC.

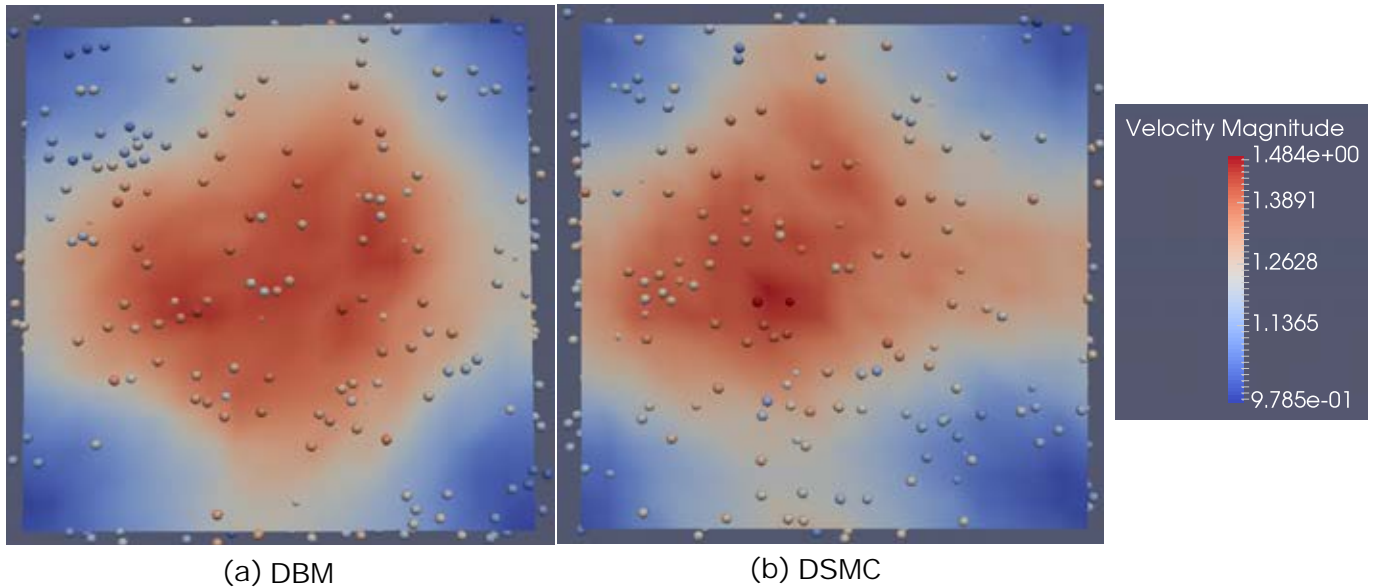


**Figure 9:** Instantaneous velocity profile after  $t = 10s$  in the x-y plane, DBM vs DSMC.

serve how bubbles behave in the bulk with different collision schemes and also the collision frequency at different transitioning velocity regimes which is important for a proper verification of the DSMC.

**Table 3:** Parameter space for 3D periodic bubble rise.

Case	Bubble size [mm]	Number of bubbles in domain [-]	Overall gas fraction ( $\epsilon_b$ ) [-]
1	2	5000	0.02

It can be observed from figures 7 and 8 that the DSMC model captures all the major phases of the bubble rise process. The different phases mainly refer to the changes in the structure of the system based on the bubble positions. The initial cubic arrangement in the system (see figure 4) breaks and homogenizes into a random arrangement as the simulation progresses. Since the bubble velocities change with time, it also has an effect on the collision frequency. The sudden rise in the collision frequency near time  $t = 1s$  is due to cluster formation of bubbles with memory of the initial configuration. Then the bubbles start layering and finally at higher velocities they homogenize, losing the memory of the initial configuration completely. The collision frequency starts decreasing after  $t = 4s$  because of the homogenization and constantly changing velocities due to accelerated liquid motion. The deviation in the collision frequency at higher velocities is due to slight over-compensation of the collisions in DSMC.

A high velocity core is observed in the velocity profile normal to the z-direction due to the biased initial configuration in the DBM (see figure 9). This effect is also well captured by the DSMC. When comparing DBM and DSMC results, the cores seem to be slightly shifted, but it should be emphasized that these are instantaneous snapshots, which are expected to be different for different sequences of bubble collisions (the so-called butterfly effect). When taking time averages the results are almost indistinguishable between the two methods.

The overall gas fraction is quite small. During the clustering the local gas volume fractions have reached up to 20 percent. A similar system with bubble size 4 mm is also simulated. The 4 mm system is much denser, therefore it reaches high velocities much faster than the 2 mm system. The collision frequency and total collisions match similar to the 2 mm case. The local gas fractions have reached values up to 39 percent in the 4 mm case.

## CONCLUSION

The DSMC model is extended to larger dispersed objects in the order of millimeters and also dense systems (up to 30-40 % gas fraction). The model has been verified for the mono-disperse systems and is currently being extended to poly-disperse systems. The next step is to further validate the model with experimental data of real bubble columns and parallelization of the method which is to be implemented for a large scale bubble column.

## ACKNOWLEDGEMENTS

This research has been funded by the NWO TOP grant "First principles based multi-scale modeling of transport in reactive three phase flows" (716.014.001).

## REFERENCES

- BIRD, G.A. (1994). *Molecular Gas Dynamics and Direct Simulation of Gas Flows*.
- BIRD, G. (2007). "Sophisticated DSMC". *DSMC07 meeting*, 1–49. URL <http://www.gab.com.au/dsmc07notes.pdf>.
- CHAUDHARI, R.V. and RAMACHANDRAN, P.A. (1980). "Three phase slurry reactors". *AIChE Journal*, **26(2)**, 177–201. URL <http://dx.doi.org/10.1002/aic.690260202>.
- DARMANA, D., DEEN, N. and KUIPERS, J. (2006). "Parallelization of an Euler-Lagrange model using mixed domain decomposition and a mirror domain technique: Application to dispersed gas liquid two-phase flow". *Journal of Computational Physics*, **220(1)**, 216–248. URL <http://www.sciencedirect.com/science/article/pii/S0021999106002294>.

- DEEN, N.G., SOLBERG, T. and HJERTAGER, B.H. (2001). "Large eddy simulation of the Gas Liquid flow in a square cross sectioned bubble column". *Chemical Engineering Science*, **56**, 6341–6349.
- DEEN, N., VAN SINT ANNALAND, M. and KUIPERS, J. (2004a). "Multi scale modeling of dispersed gas liquid two-phase flow". *Chemical Engineering Science*, **59(8-9)**, 1853–1861. URL <http://www.sciencedirect.com/science/article/pii/S0009250904000971>.
- DEEN, N., MUDDE, R., KUIPERS, J., ZEHNER, P. and KRAUME, M. (2012). "Bubble Columns". *Ullman's Encyclopedia of Industrial Chemistry*, **6**, 359–379.
- DEEN, N.G., VAN SINT ANNALAND, M. and KUIPERS, J. (2004b). "Multi-scale modeling of dispersed gas-liquid two-phase flow". *Chemical Engineering Science*, **59(8)**, 1853–1861.
- DU, M., ZHAO, C., ZHOU, B., GUO, H. and HAO, Y. (2011). "A modified DSMC method for simulating gas-particle two-phase impinging streams". *Chemical Engineering Science*, **66(20)**, 4922–4931. URL <http://linkinghub.elsevier.com/retrieve/pii/S0009250911004477>.
- HOOMANS, B., KUIPERS, J., BRIELS, W. and VAN SWAAIJ, W. (1996). "Discrete particle simulation of bubble and slug formation in a two-dimensional gas-fluidised bed: a hard-sphere approach". *Chemical Engineering Science*, **51(1)**, 99–118.
- JAIN, D., KUIPERS, J. and DEEN, N.G. (2014). "Numerical study of coalescence and breakup in a bubble column using a hybrid volume of fluid and discrete bubble model approach". *Chemical Engineering Science*, **119**, 134–146. URL <http://www.sciencedirect.com/science/article/pii/S0009250914004448>.
- KITAGAWA, A., MURAI, Y. and YAMAMOTO, F. (2001). "Two-way coupling of Eulerian-Lagrangian model for dispersed multiphase flows using filtering functions". *International Journal of Multiphase Flow*, **27(12)**, 2129–2153.
- LAU, Y., ROGHAI, I., DEEN, N., VAN SINT ANNALAND, M. and KUIPERS, J. (2011). "Numerical investigation of the drag closure for bubbles in bubble swarms". *Chemical Engineering Science*, **66(14)**, 3309–3316.
- LUTIŠAN, J. (1995). "The treatment of molecular collisions in dsmc methods". *Molecular Simulation*, **14(3)**, 189–206.
- PATANKAR, S. (1980). *Numerical heat transfer and fluid flow*. CRC press.
- PAWAR, S., PADDING, J., DEEN, N., JONGSMA, A., INNINGS, F. and KUIPERS, J. (2014). "Lagrangian modelling of dilute granular flow modified stochastic DSMC versus deterministic DPM". *Chemical Engineering Science*, **105**, 132–142. URL <http://linkinghub.elsevier.com/retrieve/pii/S0009250913007331>.
- ROGHAI, I., LAU, Y., DEEN, N., SLAGTER, H., BALTUSSEN, M., ANNALAND, M.V.S. and KUIPERS, J. (2011). "On the drag force of bubbles in bubble swarms at intermediate and high reynolds numbers". *Chemical engineering science*, **66(14)**, 3204–3211.
- TOMIYAMA, A., MATSUOKA, T., FUKUDA, T. and SAKAGUCHI, T. (1995). "A simple numerical method for solving an incompressible two-fluid model in a general curvilinear coordinate system". *Multiphase Flow*, **95**.
- TOMIYAMA, A., TAMAI, H., ZUN, I. and HOSOKAWA, S. (2002). "Transverse migration of single bubbles in simple shear flows". *Chemical Engineering Science*, **57(11)**, 1849–1858.
- UNVERDI, S.O. and TRYGGVASON, G. (1992). "A front-tracking method for viscous, incompressible, multi-fluid flows". *Journal of computational physics*, **100(1)**, 25–37.
- VAN SINT ANNALAND, M., DEEN, N. and KUIPERS, J. (2005). "Numerical simulation of gas bubbles behaviour using a three-dimensional volume of fluid method". *Chemical Engineering Science*, **60(11)**, 2999–3011. URL <http://linkinghub.elsevier.com/retrieve/pii/S0009250905000564>.
- VREMAN, A. (2004). "An eddy-viscosity subgrid-scale model for turbulent shear flow: Algebraic theory and applications". *Physics of Fluids (1994-present)*, **16(10)**, 3670–3681.
- ZHANG, D. (2007). *Eulerian modeling of reactive gas-liquid flow in a bubble column*. phdthesis, University of Twente, Netherlands.